# MOX and UOX Fuel Melt Margin for European Pressurized Reactor

Patryk Oskar Stręciwilk, Piotr Darnowski, Adam Dominiak*, Roman Domański

*Warsaw University of Technology, Faculty of Power and Aeronautical Engineering, Institute of Heat Engineering*
*Nowowiejska 21/25, 00-665 Warsaw, Poland*

## Abstract

Safety is of paramount importance inthe design and maintenanceof Nuclear Power Plants (NPP). The crucial area is the nuclear island,where irradiated elements are located. Fuel melt is a very dangerous possibility during serious incidents in the nuclear reactor core and could lead to the release of enormous amounts of radioactive elements. Uranium Oxide (UOX) and Mixed Oxides (MOX) are currently being consideredas fuels for existing and planned NPPs. This paper addresses UOX and MOX fuel melt calculations using a prepared Thermal-Hydraulics (TH) model and reliable thermal conductivity of UOX and MOX fuel relations. This evaluation is performed for European Pressurized Reactor (EPR) geometry and thermophysical parameters.

*Keywords:* Fuel melt, Nuclear fuel, Thermal-hydraulics model

## 1. Introduction

A typical pressurized water reactor (PWR) operates on UOX fuel enriched to ca. 3–5% of fissile $^{235}_{92}U$ the remainder being non-fissile $^{238}_{92}U$. UOX, the dominating nuclear fuel today, is a well proven and reliable fuel and it is believed that its importance will remain high in existing and planned PWRs for the next few decades, especially as this uranium fissile isotope is the only one occurring in large amounts in nature. Nevertheless reactor vendors, operators and governments are looking for alternative sources of other fissile isotopes to secure the supply of nuclear energy. An attractive alternative to UOX is MOX fuel containing a composition of 5-9% fissile and non-fissile plutonium isotopes mixed with depleted or natural uranium [1, 2]. An important aspect is that the plutonium mixture for MOX fuel can be recovered from spent nuclear fuel by reprocessing methodologies and military stockpiles, including nuclear warheads. MOX fuel is currently generating about 2% of all power supplied by oxide fuels, but this figure could well rise in future [3]. At the date of writing approximately 40 reactors in Europe are licensed to use MOX fuel [4]. In current cores for safety issues the inventory of MOX assemblies cannot exceed 30%, but in planned Gen III+ reactors like AP1000 and EPR it could be 100% [3–5].

MOX fuel properties differ slightly from UOX fuel and some could be negativelysafety related. Hence, use of that fuel demands special attention in terms of reactor engineering. A keyissue is the control capabilities of soluble absorbers like boron, which are used forreactivity control and to maintain subcriticality during shutdown. Those are reduced when MOX fuel is loaded, because the neutron spectrum is hardened through the presence of resonances in the thermal energy spectrum of some plutonium isotopes and it causes less absorption in the control material

in this energy region. This leads to problems with maintaining the correct sub-criticality level during shutdown. Boron cannot be simply added in large amounts, because boric acid hasa solubility limit in water. Additionally,neutron spectrum hardening reduces the efficiency of control rods [1, 2]. Another important issue is the reduced MOX thermophysical properties compared to UOX fuel, and this problem increases especially with fuel burnup and higher content of plutonium isotopes. For the purposes of engineering analysis there is a wealth and variety of data and correlations available in the literature regarding the properties of nuclear fuels and it demands great care during the investigation of safety issues. Central to our interests are thermal conductivity and fuel melting temperature for UOX and MOX fuels.A useful overview of MOX fuel was made by Feher et al. [4].

The performance of nuclear fuel is crucial for thermal analysis of physical phenomena in the nuclear fuel element. Physical and mechanical parameter dynamics during the burnup process do change boundary conditions for the TH model. Fuel performance parameters are presented by Romano et al. [6]. Most fuel performance analyses concern fuel burnup and strategies for maximization under specified conditions and use of different fuels [7, 8].

Thermal and structural parameters of nuclear fuel are also under consideration. Rondinella and Wiss [9] present the correlation between the atomic structure of burnt fuel and the experimental results of thermal conductivity analysis for nuclear fuel pellets.

Thermal and mechanical parameters of nuclear fuel are also investigated by Walker et al. [10]. An experimental study is performed of thermal conductivity, porosity, radial burnup and various fission products.

All the recent research mentioned above confirm the statement that new, different fuels with a higher range of thermal properties during the operational period will be applied for nuclear energy.

The motivation for this work was to investigate what influence the fuel type (MOX or UOX), burnup and fuel composition have on the temperature margin to melt during steady state normal operation of a PWR nuclear reactor (for standard EPR parameters). It is clear that fuel melt margin takes on a spe-
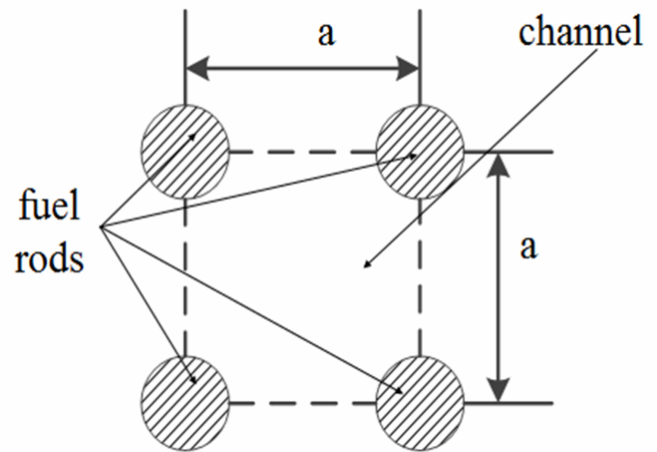


Figure 1: Single reactor cooling channel considered in analysis [12]

cial importance in accident conditions. Nevertheless, analysis for normal operation should provide insight as to what might be expected in an abnormal situation. It should be kept in mind that normal operation conditions are usually the initial conditions for accident progression. The significance of this issue is explored in Qi et al. [11]. In order to assess the thermal conditions of nuclear fuel in the reactor single cooling channel the TH model was created and implemented in computer code [12, 13]. This simplified model has been developed since the late 1960s [14].

## 2. Thermal-Hydraulics Model

One dimensional, single phase, steady state flow conservation equations are solved in the presented TH model. The reactor cooling channel is divided into a couple of equal length control volumes. The equations solved are based on the formulations described by Levy [15] and by Kazimi and Todreas [16] for the nuclear reactor cooling channel (Figure 1). The continuity equation (mass conservation) for the analyzed situation is given by Eq. (1):

$$\frac{d}{dz}\dot{m} = 0 \qquad (1)$$

This equation is correct if we assume that channel cross sectional area $A$ is constant. Moreover, the momentum conservation equation takes the form:

$$\frac{d}{dz}\left(\frac{\dot{m}^2}{\rho A}\right) = -A\frac{dp}{dz} - \overline{\tau_w}P - \rho g A \sin(\theta) \qquad (2)$$

where $P$ is wetted perimeter of the channel and $\overline{\tau_w}$ is average wall shear stress. Assuming that we analyze vertical flow only and rearranging it for pressure drop, Eq. (2) can be rewritten in the following form:

$$-\frac{dp}{dz} = \frac{1}{A}\frac{d}{dz}\left(\frac{\dot{m}^2}{A\rho}\right) + \frac{\overline{\tau_w}P}{A} + \rho g \qquad (3)$$

Equation (3) is differential equation for pressure drop across the channel: acceleration pressure drop, frictional pressure drop and hydrostatic pressure drop.

Wall shear stress is responsible for friction and the second term on the right hand side of Eq. (3) can be formulated as the well-known Darcy-Weisbach equation [15]:

$$\left(\frac{dp}{dz}\right)_{friction} = \frac{\overline{\tau_w}P}{A} = f\frac{\rho\overline{u_z}^2}{2D_h} \qquad (4)$$

where $f$—is Darcy friction factor, $\overline{u_z}$—area averaged flow velocity, $D_h$—hydraulic diameter. The Darcy friction factor was determined iteratively by the Colebrook-White equation [16, 17].

Total mass flow for one control volume is constant and it is a natural consequence of mass conservation given by Eq. (1). Hence this equation is not integrated. Nevertheless in the created computer code the density of the fluid can change due to a change in fluid temperature and change very little by a change in pressure in a given node (due to $\rho = \rho(p, T)$). Constant mass flow is the boundary which allows for the calculation of flow velocity:

$$\overline{u_z} = \frac{\dot{m}}{\rho A} \qquad (5)$$

Momentum equation Eq. (3) is solved semi-implicitly, node by node. In the axial nodes with spacer grids, inlet and outlet nozzles pressure at exit of the node is additionally reduced by pressure form loss:

$$(\Delta p)_{form} = K_i\frac{\rho\overline{u_z}^2}{2} \qquad (6)$$

where $K_i$ is loss coefficient on the nozzle or spacer grid. Energy conservation equation [15, 16]:

$$\frac{d}{dz}\left(\dot{m}\overline{h}\right) + \frac{1}{2}\frac{d}{dz}\left(\frac{\dot{m}^3}{A^2\rho^2}\right) = P_h\overline{q''} - A\overline{q'''} - g\dot{m}\sin(\theta) \qquad (7)$$

where $P_h = P$ is heated perimeter and after rearrangement, Eq. (7) is:

$$\frac{d\overline{h}}{dz} + \frac{1}{2}\frac{d}{dz}\left(\frac{\dot{m}^2}{A^2\rho^2}\right) = \frac{P_h\overline{q''}}{\dot{m}} - \frac{A\overline{q'''}}{\dot{m}} - g\sin(\theta) \qquad (8)$$

It is assumed that there is no volumetric heat source in the coolant (for example, generated by gamma radiation), potential energy and kinetic energy are negligible and only fission heat generation represented by heat flux $q''$ or linear heat rate $q'$ is relevant:

$$\frac{d\overline{h}}{dz} = \frac{P_h\overline{q''}}{\dot{m}} = \frac{\overline{q'}}{\dot{m}} \qquad (9)$$

Energy balance equation Eq. (9) is solved node by node in a similar manner to the momentum equation. It was assumed that the neutron flux has a simple chopped cosine axial profile. In consequence, the linear heat rate has the same form:

$$\overline{q'}(z) = \overline{q'}_0 \cos\frac{\pi z}{H_e} \qquad (10)$$

where $H_e$ is extrapolation length for neutron flux. This value was assumed to be 10 cm, which is quite a reasonable approximation for such a model. Cosine power/flux profile occurs only for a bare cylindrical core without a reflector and it is a strong simplification [16]. Nevertheless for Beginning of Cycle in an EPR reactor this profile has a more or less cosinusoidal shape [18].

The TH model derived above represents an external iteration of the whole code and is mainly dedicated to determining axial changes of coolant properties. In contrast, internal iteration is used to find radial distribution of temperatures in the fuel elements to find axial profiles of fuel, gas gap and cladding temperatures. It was assumed that there is no axial heat transfer in the fuel.

When pressure and enthalpy in the control volume are known, average temperature, density, viscosity,

thermal conductivity and specific heat capacity (denoted as $f_{fl}(z)$) are determined using steam-water tables:

$$f_{fl}(z) = f(p(z), h(z)) \qquad (11)$$

Steam-water properties were based on the IAPWS IF-97 formulation implemented in the X-Steam package [19]. Based on those tables the Reynolds and Prandtl numbers for any given node can be obtained:

$$Re = \frac{\rho \overline{u_z} D_h}{\mu}, \quad Pr = \frac{c_p \mu}{k_c} \qquad (12)$$

The Nusselt number is required for the purposes of calculating the heat transfer coefficient between coolant and cladding surface. Flow in reactor channel in steady state is generally turbulent and the Nusselt number can be obtained by Gnielinski correlation [17]:

$$Nu = \frac{(f/8)(Re - 1000) Pr}{1 + 12.7 \left(\frac{f}{8}\right)^{0.5} (Pr^{2/3} - 1)} \qquad (13)$$

and consequently the heat transfer coefficient for the cladding-coolant interface:

$$h_{cs} = Nu \frac{k_w}{D_h} \qquad (14)$$

Temperature on the outside surface of the cladding is [16]:

$$T_{so} = T_{fl} + \frac{\overline{q'}}{2\pi h_{cs}(r_F + t_G + t_C)} \qquad (15)$$

where $r_F$ is fuel pellet radius, $t_G$ gas gap thickness and $t_C$ cladding thickness. Cladding surface inner temperature is given by expression [16, 20]:

$$T_{si} = T_{so} + \frac{\overline{q'}}{2\pi k_C} \ln \left( \frac{r_F + t_G + t_C}{r_F + t_G} \right) \qquad (16)$$

where $k_C$ is cladding thermal conductivity, which was assumed to be constant. Moreover temperature $T_G$ on the outside surface of the fuel pellet is governed by assumed heat transfer coefficient of gas gap $h_G$:

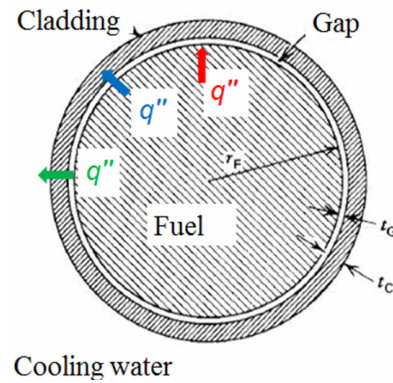$$T_G = T_{si} + \frac{\overline{q'}}{2\pi r_F h_G} \qquad (17)$$



Figure 2: Single square cell [12]

Thermal conductivity of the fuel can strongly differ with radius, due to the very high temperature gradient in oxide fuels. Hence, conductivity integral should be computed in order to find the precise fuel centerline temperature [16]:

$$\int_{T_G}^{T_{CL}} k_F(T) \, dT = \frac{\overline{q'}}{4\pi} \qquad (18)$$

Nevertheless, unknown temperature is in integral boundary and the iterative process was applied to equate left and right hand side of Eq. (18). Simpson Quadrature was the integration method used.

The conductivity integral is fuel geometry non-dependent and the main role is played by fuel thermal conductivity correlation, linear heat and lower integral limit [16].

## 3. UOX and MOX Thermal Conductivity and Melting Temperature Correlations

Generally, UOX and MOX thermal conductivity correlations consist of two parts: the first (for lower temperatures) decreasing with temperature and the second (for higher temperatures) increasing with temperature. The thermal conductivity value for standard models reaches its minimum at ca. 1900 K for both UOX and MOX fuels. Thermal conductivity values for UOX fuels are slightly higher than for MOX fuels across the whole temperature range. Moreover, the fuel thermal conductivity correlations are strongly related to the fuel burnup. In the physical model use was made of correlations for UOX and MOX proposed by Carbajo et al. [21] based on the general relation:
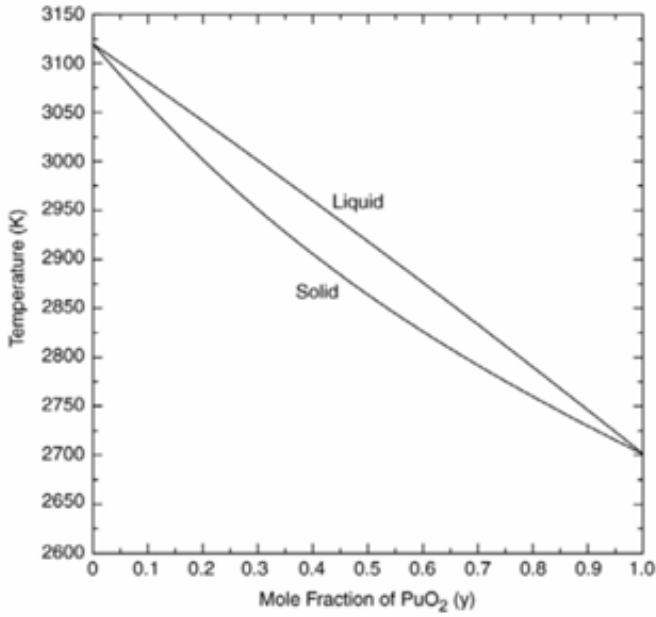
Figure 3: Solidus and liquidus phase lines for UOX and MOX mixtures [19, 20]



Figure 4: Melting temperatures for different UOX and MOX burnup [21]

$$k_F(T, B, x, p) =$$
$$k_0(T, x) FD(B, T) FP(B, T) FM(p) FR(T) \tag{19}$$

$k_0$ is the basic expression for unirradiated substance with no porosity ($t = T/1000$ and $x$ is deviation from stoichiometry):

$$k_0(T, x) = \frac{1}{0.0257 + 3.336x + \frac{(2.206 - 6.85x)t}{10}} + 1.158 \cdot \frac{6400}{t^{\frac{5}{2}}} e^{-\frac{16.35}{t}} \tag{20}$$

FD and FP in Eq. (19) relies on burnup, FM on porosity. Radiation effect FR was omitted because it is not dependent on burnup and sharply decreases at temperatures over 900 K.

The solidus state boundary temperature relation for the UO2-PuO2 ceramic mixture is reported by Adamson et al. [22] (Fig. 3).

Temperature dependence as well as burnup effect is applied for thermal conductivity and UOX and MOX melt temperature correlations (Fig. 4). Fuel porosity is set as 5% which is in linewith real cases [1] and deviation from theoretical density which thermal conductivity and melting point correlations describe [22–24].
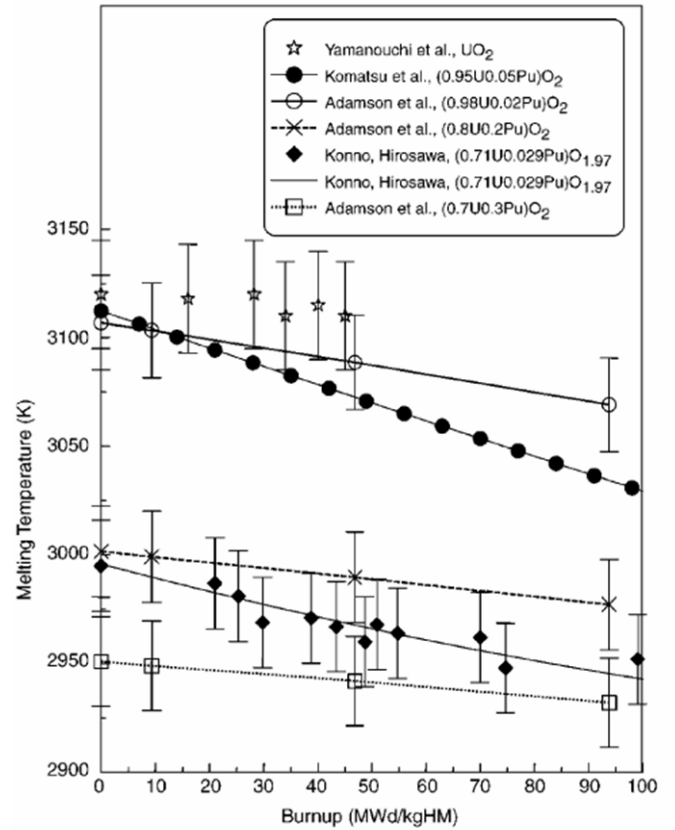
## 4. Calculations and Results

Parameters and geometry for coolant, channel and fuel rods are presented below [15, 25]. These are as per the EPR made by Areva:

- coolant temperature at the inlet to the channel $T_{inlet} = 568.9$ K,

- coolant pressure at the inlet to the channel $p_{inlet} = 155$ bar,

- channel length $H = 4.2$ m,

- mean linear power density $\overline{q'} = 15.61 \frac{kW}{m}$,

- fuel pellet diameter $d_F = 8.19$ mm,

- gas gap thickness $t_G = 0.084$ mm,

- fuel cladding thickness $t_C = 0.57$ mm,

- lattice pitch $a = 12.6$ mm,

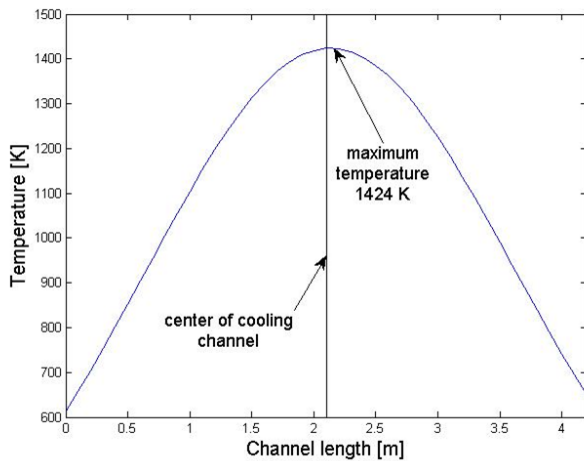- cladding thermal conductivity $k_C = 10.7 \frac{W}{mK}$,

Figure 5: Temperature distributionin fuel pellet center with location of maximum temperature

- gas gap heat transfer coefficient $h_G = 5000 \frac{W}{m^2 K}$.

In modern nuclear fuel solutions for Pressurized Water Reactors $PuO_2$ content does not exceed 9% [3]. Thermal properties correlations available in the literature allow one to prepare a fuel melt margin analysis for 0% $PuO_2$ in fuel (i.e. pure $UO_2$), 2% $PuO_2$ in fuel and 5% $PuO_2$ in fuel.

The TH model in the nuclear reactor cooling channel was resolved for nine different cases: all types of fuel mentioned above with burnup at the level of 0, 50 and 100 MWd/kgHM. For all cases the highest temperature inside the fuel element was determined (from the numerical model) as well as the melting temperature (from the data presented in Fig. 4). The maximum temperature in the fuel pellet is slightly above the medium of the fuel rod, which is presented in Fig. 5. The melt margin results are presented in Tab. 1. In the model sufficient fuel thermal conductivity equations were used [21].

As to the present fuel melt margin,the highest temperature in the fuel pellet and the fuel melt temperature for all cases were determined. The difference between the two temperatures is the fuel melt margin and is presented in Fig. 6 for all cases included.

## 5. Conclusions

The difference in thermal conductivity in UOX and MOX fuels directly influences temperature distribution inside the nuclear fuel rod. Moreover, ther-

Table 1: Centerline pellet maximum temperature and melting point of fuel pellet for different fuel types and burnup

| Fuel type | $PuO_2$ fraction | Burnup, $\frac{MWd}{kgHM}$ | Centerline pellet maximum temperature, K | Melting point, K |
|---|---|---|---|---|
| UOX ($UO_2$) | 0 | 0 | 1424 | 3120 |
| | 0 | 50 | 1422 | 3095 |
| | 0 | 100 | 1420 | 3070 |
| MOX 2% $PuO_2$ | 0.02 | 0 | 1603 | 3107 |
| | 0.02 | 50 | 1601 | 3082 |
| | 0.02 | 100 | 1599 | 3057 |
| MOX 5% $PuO_2$ | 0.05 | 0 | 1738 | 3088 |
| | 0.05 | 50 | 1736 | 3063 |
| | 0.05 | 100 | 1734 | 3038 |

mal conductivity for both fuels differs slightly with fuel burnup. As a result the difference between the maximum temperature of the fuel pellet and its melting point (melt margin) differs for each analyzed case.

As presented in Fig. 6 the highest melt margin there is for pure uranium fuel and decreases as the $PuO_2$ fraction in the fuel rises. As the thermal conductivity and melting point are influenced by fuel burnup, this parameter also changes the melt margin.

For fuels with no burnup the melt margin decreases with the $PuO_2$ fraction from 1696 K for pure $UO_2$ to 1350 K for 5% $PuO_2$. The melt margin for these cases differs by 346 K.

The melt margin between fresh fuel and fuel with burnup value 100 MWd/kgHM is ca. 46 K and is similarfor all kind of analyzed fuels.

It is necessary to mention that burnup of 100 MWd/kgHM is unattainable for PWR (the US Nuclear Regulatory Commission mandates that maximum fuel burnup must be below 62 MWd/kgHM [26]), but the analyses were made to present the trend for all fuel types.

Further studies should investigate more accurate linear power density profiles for different moments of the fuel cycle. This is because power peaks could
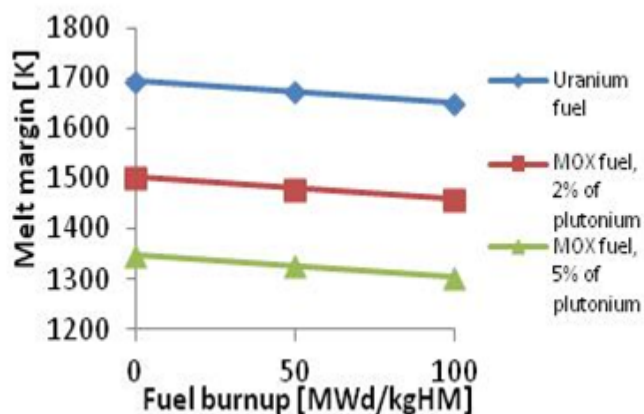
Figure 6: Difference between melting temperature and highest temperature in pellet for different fuel types changing with fuel burnup

occur which might in turn lead to lower fuel melt margins.

To sum up, the change of fuel in the nuclear assembly definitely alters the temperature distribution inside the fuel rod and the cooling channel. This difference can have a major impact on thermal stresses and water boiling parameters, which need to be carefully analyzed before changing fuel type in the nuclear reactor core.

A change of fuel leads to a change in the fuel melt margin in steady state normal operation. In consequence, this could lead to a difference which could have a major impact on the initial conditions of the nuclear fuel state during any nuclear incident.

## References

[1] J. Wallenius, Transmutation of Nuclear Waste, KTH, Blykalla böcker och spel, 2011.

[2] H. R. Trellue, Safety and neutronics: A comparison of mox vs uo2 fuel, Progress in Nuclear Energy 48 (2006) 135–145.

[3] J. Zakova, Advanced fuels for thermal spectrum reactors, Ph.D. thesis, KTH Reactor Physics Division, Stockholm, Sweden (2012).

[4] S. Feher, T. Reiss, A. Wirth, Mox fuel effects on the isotope inventory in lwrs, Nuclear Engineering and Design 252. doi:10.1016/j.nucengdes.2012.06.035.

[5] P. C. Burns, R. C. Ewing, A. Navrotsky, Nuclear fuel in a reactor accident, Science 335. doi:10.1126/science.1211285.

[6] A. Romano, C. A. Shuffler, H. D. Garkisch, D. R. Olander, N. E. Todreas, Fuel performance analysis for pwr cores, Nuclear Engineering and Design 239. doi:10.1016/j.nucengdes.2008.11.022.

[7] Z. Xu, Design strategies for optimizing high burnup fuel in pressurized water reactors, Ph.D. thesis, Massachusetts Institute of Technology (2003).

[8] L. Yun, Modeling the performance of high burnup thoria and urania pwr fuel, Ph.D. thesis, Massachusetts Institute of Technology (2002).

[9] V. V. Rondinella, T. Wiss, The high burn-up structure in nuclear fuel, Materials Today 13. doi:10.1016/S1369-7021(10)70221-2.

[10] C. T. Walker, D. Staicu, M. Sheindlin, D. Papaioannou, W. Goll, F. Sontheimer, On the thermal conductivity of uo2 nuclear fuel at a high burn-up of around 100 mwd/kghm, Journal of Nuclear Materials 350. doi:10.1016/j.jnucmat.2005.11.007.

[11] Y. Qi, P. Henningson, J. Strumpell, S. H. Shann, The effect of fuel thermal conductivity degradation with burnup on pwr licensing limits, in: 18th International Conference on Nuclear Engineering, 2010.

[12] P. O. Stręciwilk, P. Darnowski, A. Dominiak, Nuclear reactor cooling channel thermal-hydraulics numerical model implemented in matlab environment, in: Nuclear Power Development: A Challenge for Science and Industry Conference Mądralin 2013, Warsaw, 2013.

[13] P. O. Stręciwilk, Construction of a simplified thermal-hydraulics numerical model in PWR nuclear reactor core, BSC thesis, Warsaw University of Technology (2013).

[14] R. Nijsing, Temperature and heat flux distribution in nuclear fuel element rods, Nuclear Engineering and Design 4.

[15] S. Levy, Two-Phase Flow in Complex Systems, John Wiley & Sons Inc., 1999.

[16] M. S. Kazimi, N. E. Todreas, Nuclear Systems I: Thermal Hydraulic Fundamentals, 3rd Edition, Taylor and Francis, Levittown, 1993.

[17] Y. A. Cengel, Heat and mass transfer: a practical approach, 3rd Edition, McGraw-Hill, New York, 2006.

[18] Areva, U.S. EPR Application Documents, FSAR, Tier 2, Chapter 4.3: Nuclear Design.

[19] M. Holmgren, X-Steam, Thermodynamic properties of water and steam, 2007 MATLAB Steam-Water Tables based on IAPWS IF-97.

[20] H. Anglart, Thermal-Hydraulics in Nuclear Systems, 1st Edition, Institute of Heat Engineering Warsaw University of Technology, Warsaw, 2013.

[21] J. J. Carbajo, G. L. Yoder, S. G. Popov, V. K. Ivanov, A review of the thermophysical properties of mox and uo2 fuels, Journal of Nuclear Materials 299. doi:10.1016/S0022-3115(01)00692-4.

[22] M. G. Adamson, E. A. Aitken, R. W. Caputi, Experimental and thermodynamic evaluation of the melting behavior of irradiated oxide fuels, Journal of Nuclear Materials 130. doi:10.1016/0022-3115(85)90323-X.

[23] C. Ronchi, M. Sheindlin, M. Musella, G. J. Hyland, Thermal conductivity of uranium dioxide up to 2900

k from simultaneous measurement of the heat capacity and thermal diffusivity, Journal of Applied Physics 85. doi:10.1063/1.369159.

[24] J. Komatsu, T. Tachibana, K. Konashi, The melting temperature of irradiated oxide fuel, Journal of Nuclear Materials 154. doi:10.1016/0022-3115(88)90116-X.

[25] Framatome ANP, EPR (2005).

[26] Boston Consulting Group, Economic Assessment of Used Nuclear fuel Management in the United States (2006).

**Nomenclature**

$\dot{m}$ — mass flow, $\frac{kg}{s}$

$(\Delta p)_{form}$ — pressure form loss, bar

$\mu$ — dynamic viscosity, $\frac{kg}{s \cdot m}$

$\overline{\tau_w}$ — average wall shear stress, Pa

$\overline{h}$ — mean specific enthalpy, $\frac{J}{kg}$

$\overline{q'_0}$ — average peak linear power density, $\frac{W}{m}$

$\overline{q'}$ — average linear power density, $\frac{W}{m}$

$\overline{q'}$ — average volumetric power density, $\frac{W}{m^3}$

$\overline{u_z}$ — average flow velocity in cooling channel, $\frac{m}{s}$

$\rho$ — coolant density, $\frac{kg}{m^3}$

$\theta$ — the slope of the channel, -

$A$ — cooling channel cross section, m$^2$

$a$ — fuel rods spacing, mm

$B$ — burnup, atomic percent [at.%] or/and $\left[\frac{MWd}{tHM}\right]$

$c_p$ — coolant specific heat, $\frac{J}{kg \cdot K}$

$d_F$ — fuel pellet diameter, m

$D_h$ — hydraulic diameter, m

$f$ — friction factor, -

$FD$ — factor for effect of dissolved fission products, -

$FM$ — factor for fuel porosity, -

$FP$ — factor for effect of precipitated fission products, -

$FR$ — factor for effect of radiation damage, -

$g$ — gravitation constant, $\frac{m}{s^2}$

$H$ — cooling channel length, m

$h_{cs}$ — convection heat transfer coefficients on cladding surface, $\frac{W}{m^2 K}$

$H_e$ — extrapolation length, m

$h_G$ — heat transfer coefficient in gas gap, $\frac{W}{m^2 K}$

$K$ — spacer grid pressure drop coefficient, -

$k_0$ — fuel pellet thermal conductivity, basic expression, $\frac{W}{m \cdot K}$

$k_C$ — cladding thermal conductivity, $\frac{W}{m \cdot K}$

$K_F$ — fuel thermal conductivity, $\frac{W}{m \cdot K}$

$k_w$ — water thermal conductivity, $\frac{W}{m \cdot K}$

$Nu$ — Nusselt number, -

$P$ — wetted perimeter of the channel, m

$p$ — pressure, bar

$P_h$ — heated perimeter, m

$p_{inlet}$ — pressure channel inlet, bar

$Pr$ — Prandtl number, -

$r_F$ — fuel pellet radius, m

$Re$ — Reynolds number, -

$T_{CL}$ — fuel temperature in its axis, K

$t_C$ — cladding thickness, m

$T_{fl}$ — cooling water temperature in cooling channel axis, K

$T_G$ — external fuel pellet surface temperature, K

$t_G$ — gas gap thickness, m

$T_{inlet}$ — cooling water inlet temperature, K

$T_{si}$     internal cladding temperature, K

$T_{so}$     external cladding surface temperature, K

$x$     deviation from stoichiometry,